Rotational Characterization of an n→π* Interaction in Pyridine-Formaldehyde Adduct

*Susana Blanco and Juan Carlos López**

Departamento de Química Física y Química Inorgánica, Facultad de Ciencias, Universidad de Valladolid, E-47011 Valladolid, Spain.

AUTHOR INFORMATION

Corresponding Author

* E mail: jclopez@qf.uva.es

ABSTRACT

The rotational spectrum of the pyridine–formaldehyde adduct generated in a supersonic expansion has been analyzed using Fourier transform microwave spectroscopy. The spectrum shows the quadrupole coupling hyperfine structure due to the presence of ^{14}N. The spectra of the parent, ^{13}C and ^{15}N isotopologues have been observed to investigate its structure. The complex shows a C_s symmetry with the plane of pyridine bisecting the ∠HCH angle of formaldehyde and the N atom located along the Bürgi-Dunitz trajectory of nucleophile addition to a carbonyl group (r(N-C)= 2.855(4) Å, ∠NC=O=102.8(6)º). From this structure and with the help of ab initio computations and natural bond orbital analysis it is shown unambiguously that pyridine links to formaldehyde, the smallest molecule bearing a carbonyl group, through an n→π* interaction together with a weak C-H···O bond.

TOC GRAPHICS

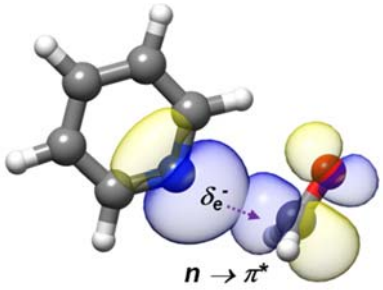

Non-covalent interactions are responsible for processes like solvation or molecular recognition and modulate the structure, function and dynamics of biomolecules. While hydrogen bond (HB) is probably the best known of such interactions[1,2] much less attention has been paid to other types of interactions like for example those involving a nucleophile and a carbonyl group.[3,4] In their seminal works, Bürgi and Dunitz[5–7] identified those interactions, observed from crystal structure survey analysis, as the experimental basis for mapping the reaction coordinate for the addition of oxygen or nitrogen nucleophiles to a carbonyl group (see Figure 1). They report that at large distances the main interaction would occur between local dipoles of the nucleophile and the carbonyl group. However, at short distances the carbonyl group appears to adopt a pyramidal shape indicating that for close contacts orbital overlap becomes important.[5] Following this description, nucleophile-carbonyl group interactions have been called orthogonal multipolar interactions[3] when the structure of the carbonyl group does not evidence significant deformations. However, it has been shown that even in those cases orbital overlap and electron density transfer should be taken into account (see Figure 1).[4,8,9] In this way those nucleophile-carbonyl group contacts can be considered to form part of the so called $n\rightarrow\pi^*$ interactions including nucleophile contacts with different kind of acceptors.[10] When the acceptor is a carbonyl group it involves the delocalization of a lone pair (n) of the nucleophile donor group into the antibonding (π^*) orbital of the carbonyl group.[4]

Crystal structure analysis and database searches have led to the identification of many contacts attending to this interaction picture for different kind of nucleophiles including C=O itself, halogen atoms and groups containing N, O, S or P.[3] These contacts have been recognized to play an important role in stabilizing the structure of biomolecules.[3,4,10–12] Signatures of those counter-intuitive $n\rightarrow\pi^*$ interactions are: (i) a short contact between the donor atom and the acceptor

carbonyl carbon, allowing for orbital overlap; (ii) the location of the donor atom along the Bürgi-Dunitz[5] trajectory which maximizes n-π^* orbital overlap; (iii) pyramidalization of the acceptor group.

Rotational spectroscopy studies have shown that $n \rightarrow \pi^*$ interactions take place also in small biomolecules and complexes. For example they contribute to stabilize the most stable conformers

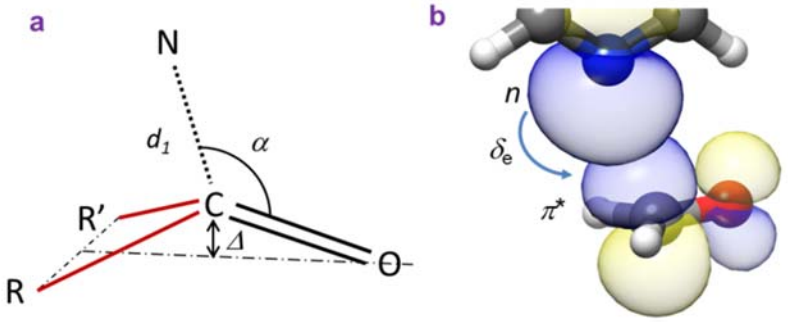

Figure 1. a) Geometrical parameters associated to an $n \rightarrow \pi^*$ interaction between a nucleophile (N) and a carbonyl group. d1 is the N···C distance (d1 ≤ $r_N + r_C$, the sum of van de Waals radii), θ is the ∠N···C=O angle (θ =107 ± 5º). For $d_1 < 3.0$ Å the approach path is predicted to lie in the plane bisecting the ∠R'CR angle. Δ reflects the displacement of the C atom from the carbonyl group plane towards the nucleophile. b) Overlap of the n donor orbital with the C=O π^* orbital.

of the neurotransmitter GABA[13] or 4(*S*)-hydroxyproline,[14] and have been observed in β-alanine,[15] 5-aminovaleric acid[16] or aspirin.[17,18] The $n \rightarrow \pi^*$ interactions between water and the carbonyl group has been shown also to cooperate with medium and weak HBs to stabilize the microsolvated adducts of β-propiolactone.[19] Complexes stabilized by the so called lone pair···π-hole interaction between water or ammonia with fully halogenated alkenes[20,21] or aromatic compounds[22] have also been detected by rotational spectroscopy. Theoretical and experimental studies of charge transfer $n \rightarrow \pi^*$, $\sigma \rightarrow \pi^*$, $\pi \rightarrow \pi^*$ complexes have been described by Weinhold and Landis.[23] However, up to the present no microwave investigations have been reported on $n \rightarrow \pi^*$ adducts for which an interaction between a nucleophile and a carbonyl compound is the main stabilization force. The

characterization of such adducts is the best way to investigate the nature of these counterintuitive $n \rightarrow \pi^*$ interactions since in most molecules one may wonder if those close contacts are the result of the optimization of the arrangement of the different parts of the molecule.

In pyridine (PY, C_5H_5N), the N atom has the structure of an imine with enhanced stability due

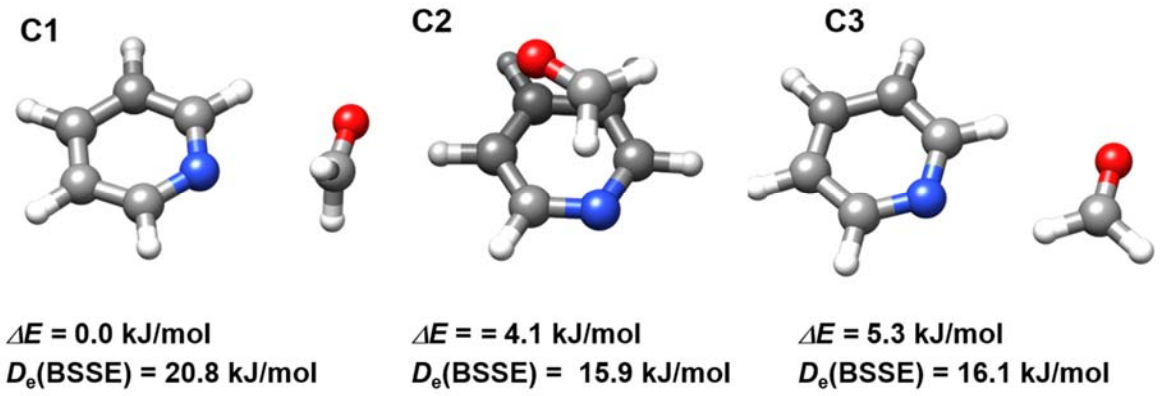

Figure 2. Shapes and energies of some stable forms of the adduct pyridine-formaldehyde calculated at MP2/aug-cc-pVTZ level.

to aromaticity. The axis of the N lone pair, as conventionally envisaged, is in the plane of the ring. Although rather unreactive due to aromaticity, PY or its derivatives can be used as a nucleophilic catalyst in acylation reactions.[24,25] Thus the structures of pre-reactive intermediates formed by PY and different carbonyl compounds are expected to be located along the Bürgi-Dunitz trajectory, showing the signatures of the formation of $n \rightarrow \pi^*$ interactions. To test this hypothesis we have studied the rotational spectrum of the complex formed in a supersonic expansion between PY and the simplest carbonyl system, formaldehyde (CH_2O. FA). Both molecules are good HB acceptors but weak HB donors. In this way, strong or moderate HB are avoided so a weak interaction such as that $n \rightarrow \pi^*$ could be observed.

Before collecting the spectra, full geometry optimizations of plausible forms of the complex have been done using *ab initio* calculations at different levels. We initially used BLYP-D3/6311++G(d,p) level but given the role of dispersion forces in this system we have extended the calculations using MP2 method with 6-311++G(2d,p) and aug-cc-pVTZ basis sets. In the final step we test the use of CCDST/6-311++G(2d,p) method to calculate the structure of the most stable conformer (see Table S1 and Figure S1 of the supplementary material). The initial geometries for

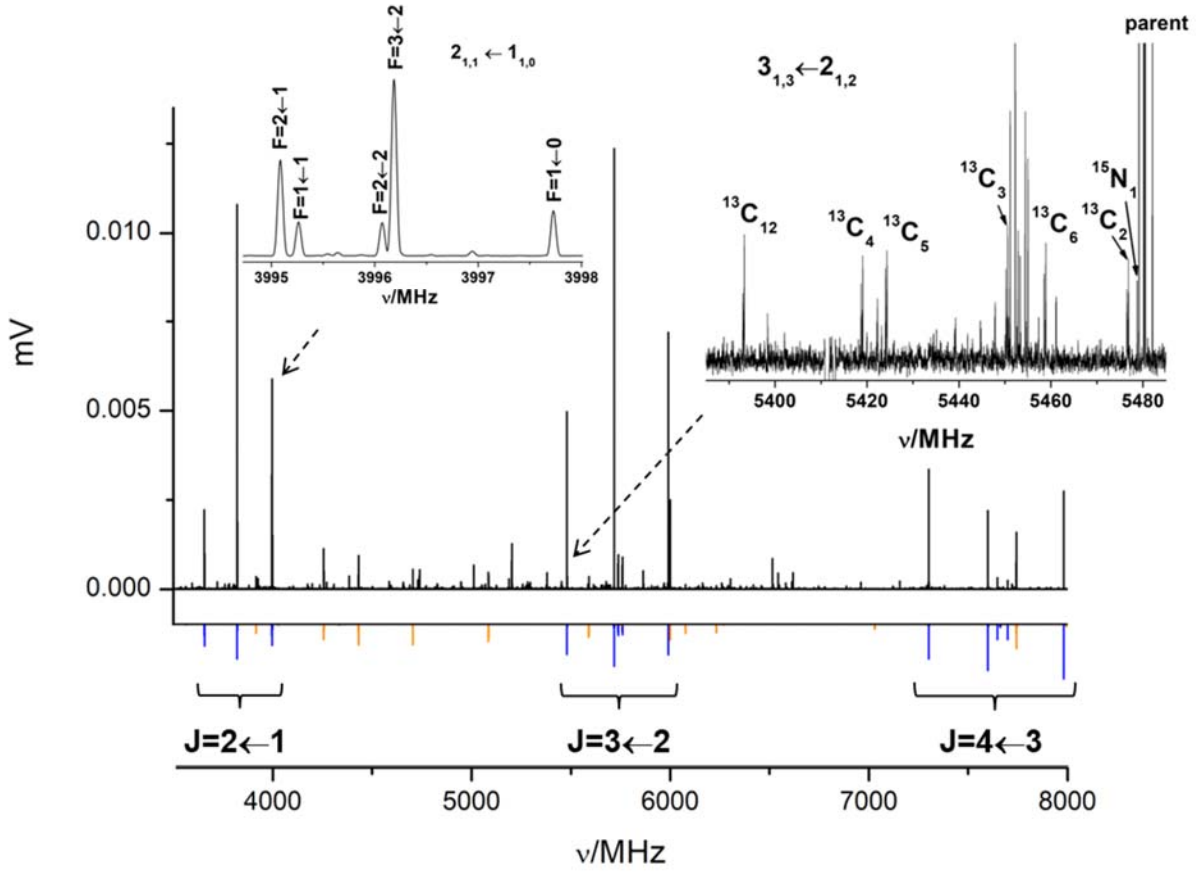

Figure 3. The CP-FTMW spectrum of the pyridine-formaldehyde complex (upper trace) compared to the predicted spectrum (lower trace). The spectrum was collected from three experiments covering the ranges 2-4 GHz, 4-6 GHz and 6-8 GHz. The observed intensities reflect the fact that the optimal operation frequency of the polarization amplifier used is 2-6 GHz. The predicted μ_a-type spectrum is plotted in blue and the μ_b-type one in orange. The excerpts show the quadrupole hfs (left) and the isotopologues in their natural abundance (right).

the six conformers found were considered following chemical intuition to test the different interaction possibilities. The conformers were labelled as CI, being I a number indicating the order of increasing energy. The three lowest energy conformers labelled C1-C3 are shown in Figure 2 together with their MP2/aug-cc-pVTZ relative (ΔE) and complexation energies D_e(BSSE), calculated taking into account basis set superposition error (BSSE).[26] These represent three different forms of interaction between both subunits. In conformer C1 an $n\rightarrow\pi^*$ interaction can be envisaged, in form C2 the two subunits are stacked and in form C3 two weak C-H···N and C-H···O take place.

The broadband FTMW spectrum of PY-FA with all known signals from formaldehyde or PY deleted is shown in Figure 3. Three groups of μ_a–type R-branch transitions spaced by B+C dominate the spectrum. Less intense μ_b–type lines can also be observed. The transitions show the quadrupole coupling hyperfine structure (hfs) due to the presence in PY of ^{14}N nucleus (see Figure 3). The spectroscopic constants, $\chi_{\alpha\beta}$ ($\alpha,\beta = a,b,c$), which are related to the coupling of the ^{14}N nuclear quadrupole moment (**I**=1), eQ, with the electric field gradient, q, at N nucleus[27] are practically a direct measure of the electric field gradient tensor elements at the nitrogen nuclei ($\chi_{\alpha\beta} = eQq_{\alpha\beta}$). The analysis[28] of the spectrum was done using a Hamiltonian including semirigid rotor[29] and quadrupole coupling[27] terms. The intensity of the μ_a–type R-branch lines allows to observe the spectra of ^{13}C and ^{15}N isotopologues in their natural abundance (see Figure 3). These were analyzed in the same way as the parent species spectrum.

Table 1. Rotational parameters obtained from the analysis of the rotational spectra of pyridine-formaldehyde adduct compared to the B3LYP-D3/6-311++G(d,p) (C1(1)), MP2/6-311++G(2d,p) (C1(2)), MP2/aug-cc-pVTZ (C1(3)) and CCSDT/6-311++G(2d,p) (C1(4)) calculated constants for the most stable form of the complex. A complete list of the observed parameters is given in Table S2.

Parameters[a]	Exp. Value	C1(1)	C1(2)	C1(3)	C1(4)
A/MHz	5128.23758(17)[b]	5147	5123	5138	5145
B/MHz	1041.53797(27)	1105	1086	1114	1039
C/MHz	871.41313(27)	915	902	921	870
1.5(χ_{aa})/MHz	-5.4503(12)	-6.02	-5.56	-5.42	-5.79
0.25(χ_{bb}-χ_{cc}) /MHz	-0.73351(48)	-0.68	-0.74	-0.77	-0.77
χ_{ab} /MHz	2.302(89)	2.31	2.28	2.17	2.43
n	249				
σ/kHz	2.3				
Derived Parameters					
P_c /uÅ2	1.90934(54)	1.76	1.77	1.75	1.77
χ_{zz}/MHz	-4.686(67)	-4.52	-4.72	-4.58	-4.94
χ_{yy}/MHz	1.402(67)	1.56	1.39	1.23	1.48
χ_{xx}/MHz	3.2838(14)	3.35	3.34	3.35	3.48
θ_{az}/° [c]	24.57(55)	22.8	24.1	24.1	24.45

[a] *A*, *B* and *C* are rotational constants χ_{aa}, χ_{bb}, χ_{cc}, χ_{ab} are ^{14}N nuclear quadrupole coupling constants. n is the number of quadrupole hfs components fitted. σ is the rms deviations of the fit. P_c is a planar moments of inertia derived from the moments of inertia I_α as $P_c=(I_a+I_b-I_c)/2$. χ_{xx}, χ_{yy} and χ_{zz} are the elements of the quadrupole coupling tensor set up in its principal axis system (*x*, *y*, *z*) [b] Standard errors are given in parentheses in units of the last digit. [c] Angle between the *a* principal inertial axis and the *z* principal quadrupole coupling axis of the pyridine-formaldehyde adduct calculated from diagonalization of the quadrupole coupling tensor.

The measurements were completed on the narrowband MB-FTMW spectrometer that has higher sensitivity and resolution. A summary of the results of the final fit for the parent species is given in Table 1. The complete results and all the measured frequencies are given in Tables S2-S11. The comparison of the experimental spectroscopic parameters (Table 1) with those calculated at different theoretical levels (see Tables 1 and S1) lead to a first identification of the observed

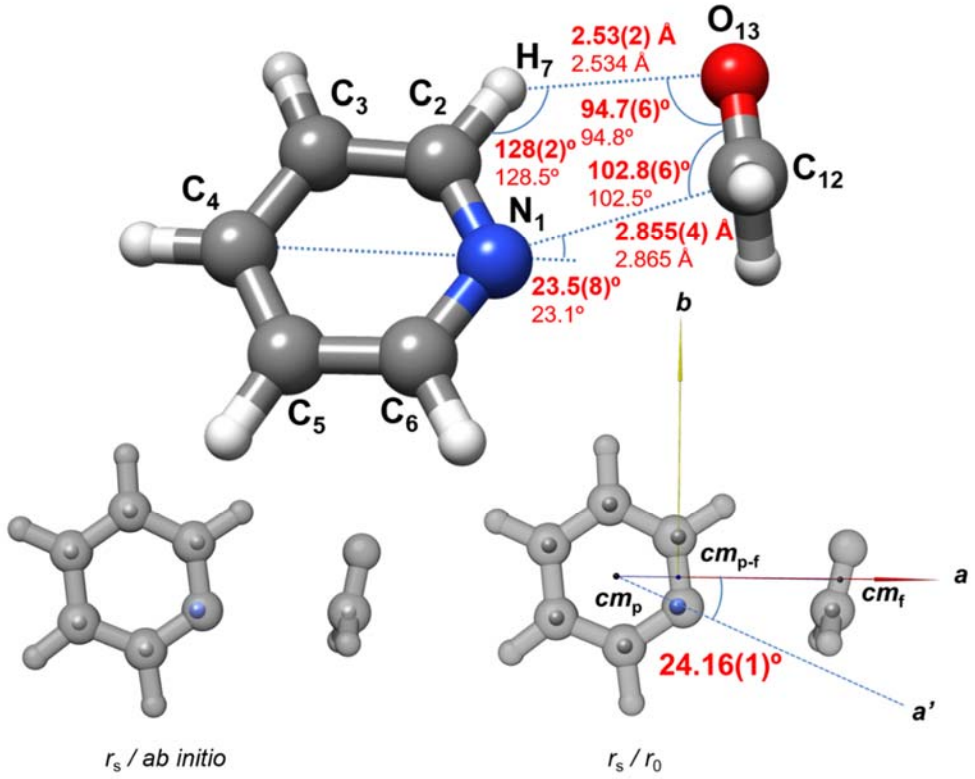

Figure 4. The structures of the pyridine-formaldehyde adduct. In the top, the r_0 non-covalent bonding distances and angles are compared with those calculated at the CCSDT/6-311++G(2d,p) level. In the bottom the r_s positions of the C and N atoms are superimposed to the *ab initio* (left) and r_0 structures (right). On the right lower figure the principal inertial axes are shown together with the line connecting the centers of mass of pyridine (cm_p), formaldehyde (cm_f) and the adduct ($cm_{p\text{-}f}$) which coincides with the *a* principal inertial axis.

conformer as conformer C1, the calculated global minimum. While the frequently used DFT or MP2 methods are useful for spectrum assignment, the best agreement between experimental and

calculated rotational constants is obtained for CCSDT/6-311++G(2d,p). Despite this, the amount and quality of our experimental data allow us to determine unambiguously the structure of the complex and reduces in this case the importance of having highly accurate quantum-chemical calculations.

The planar moment of inertia P_c giving the mass extension out of the *ab* inertial plane takes a nearly constant value of around 1.91 uÅ^2 for all the isotopologues (Tables S2-S3). This allows us to conclude that the C and the N atoms of PY and the C atom of FA are in the *ab* inertial plane. Given the planarity of PY (P_c=-0.019 uÅ^2),[30] the comparison of this value with that of ~1.82 uÅ^2 for the planar moment P_b of FA[31] (see Table S12) indicates that the *ab* plane of the adduct is coincident with the *ab* plane of PY and the *ac* plane of FA. This means that the oxygen atom of FA is also in the *ab* inertial plane of the complex with only the FA hydrogen atoms out of this plane. The small difference of 0.09 uÅ^2 can be attributed to out-of-plane intermolecular vibrational contributions. Other combinations of inertial or planar moments (see Table S12) show that FA is located not far from the *a* axis or the *ac* plane of PY.

The r_s substitution method of Kraitchman[32] is a purely experimental approach that allows to locate directly the substituted atoms of a molecule or adduct leading to the eventual unambiguous identification of a given complex. It gives the absolute values of the substituted atom coordinates in the principal inertial axis system of the parent molecular system. The signs of the coordinates can be taken from a resonable molecular structure. However the r_s method poses limitations for light atoms or for atoms located near the principal axes. An alternative way to using multi-isotopic information is to get the bond distances and angles from a least squares fit of all of the available rotational parameters[33] to determine an effective ground state, r_0, structure. The results of the application of both r_s and r_0 methods are given in Tables S13-S16 where they are compared with

the *ab* initio structure for conformer C1. These results are summarized in Figure 4. With the exception of the CCSDT, which nicely reproduces the experimental structure, theoretical methods predict shorter PY-FA distances than those found experimentally

A second source of structural data, independent of the rotational constants is the ^{14}N quadrupole coupling tensor. The complete tensor in the principal inertial axis representation (*a*, *b, c*) has been determined (see Table 1). It has only a non-zero off-diagonal element, χ_{ab}. The *c* inertial axis is parallel to one of the principal quadrupole coupling axis, let's say *x*, so $\chi_{cc} = \chi_{xx}$. The diagonalization to transform the tensor into the principal quadrupole coupling axis (*x*, *y*, *z*) representation is achieved by the rotation of an angle $\theta_{az} = 24.57(55)^o$ around the *c* axis (see Tables 1 and S17). This is the angle between the *a* and *z* axes. In bare PY, the orientations of the principal quadrupole coupling and inertial axes coincide. Labelling the inertial axes of PY as *a'*, *b*' and *c*', the identification *a'*=z, *b'*=*y* and *c'*=*x* is immediate. Assuming that the quadrupole coupling axes do not change upon complexation the diagonalization angle θ_{az} should be coincident with that between the *a* axis of the adduct and the *a'* axis of bare PY. This angle, as determined from the r_0 structure is $\theta_{aa'} = 24.16(1)^o$ (see Figure 4). The close coincidence of these two angles further confirms the observed structure.

The intermolecular stretching motion, which leads to dissociation along the Bürgi-Dunitz trajectory, appears to be almost parallel to the a-axis of the complex. The stretching force constant has been estimated to be $k_s = 7.14$ N m^{-1} from the experimental value of the Δ_J centrifugal distortion constant within the pseudo diatomic approximation[34] on the assumption that such a motion is separated from the other molecular vibrations. Assuming that the intermolecular separation for this kind of complex can be described by a Lennard–Jones type potential approximation, the

dissociation energy has been estimated[35] as E_D=10.9 kJ/mol, a value lower than those predicted theoretically (see Table S1 and Figure 2).

Ab initio computations predict the existence of other conformers of the PY-FA complex (see Table S1). Conformers C2 and C3 have energies (see Figure 2) not very far from that of C1. A plausible reason for the non-observation of C2 or C3 is the existence of conformational relaxation from these conformers to C1 in the supersonic jet. This phenomenon depends on the nature of the carrier gas and is favored for heavy gases. For PY-FA, we have used either Ar, Ne or He with the same result, only C1 has been observed. Conformational relaxation also requires the existence of a low interconversion barrier in the path for relaxation.[36] The possible interconversion paths for PY-FA have been explored at the MP2/6-311++G(2d,p) level (see figures S2-S5). The predicted barrier for the conversion of C3 into C1 through rotation of formaldehyde around its local C_2 symmetry axis (Figure S3) is of only 1 kJ/mol. The path for interconversion of C2 into C1 (Figure S5) shows a barrier of less than 3 kJ/mol. That calculated at B3LYP-D3/6-311++G(d,p) level results to be of 0.37 kJ/mol. This discrepancy between DFT and MP2 methods, found also in the calculated relative energies of C2 form (see Table S1), could indicate that dispersion forces, not equally described by these methods, are important for this conformer. Despite the discrepancies, it can be concluded that the potential barriers in the path from C2 or C3 to C1 are low enough to quench the observation of conformer C2 and C3.

The different conformers have been further investigated using natural bond orbital (NBO)[23,37] calculations at RHF/aug-cc-pVTZ level to investigate the donor→acceptor intermolecular interactions present in those forms. The results of second-order perturbation theory analysis of the Fock matrix in the NBO basis are given in Table S18. The stabilization energies calculated by deletion-type NBO re-optimizations are also given for selected interactions. By far, the strongest

intermolecular delocalization occurs from donation of the lone pair (n) of the nitrogen atom to the π^* orbital of the carbonyl group in the global minimum conformation (C1). This $n\rightarrow\pi^*$ delocalization ($E^{(2)}$ = 28.15 kJ/mol) can be considered the dominant interaction for C1 if it is compared to the small $\pi\rightarrow\sigma^*$ ($E^{(2)}$ < 2 kJ/mol) interactions or to the $n\rightarrow\sigma(C\text{-}H)^*$ ($E^{(2)}$ = 1 kJ/mol) interaction associated to the weak C-H···O HB. Weak intermolecular $n\rightarrow\sigma(C\text{-}H)^*$ HB interactions are found also in other forms. In C3 this interaction is present for the C-H···N ($E^{(2)}$ = 6.9 kJ/mol) and C-H···O ($E^{(2)}$ = 3.5 kJ/mol) HBs. In C2 some weak $\pi\rightarrow\sigma^*$ ($E^{(2)}$ < 3 kJ/mol) intermolecular interactions between the π aromatic orbitals of pyridine and the σ^*(C=O) bond are predicted reinforcing the role that dispersion/electrostatic forces may play in this form. A comparison of the NBO calculations done at B3LYP/6-311++G(d,p) and RHF/6-311G++(2d,p) are given in Table S19 for the $n\rightarrow\pi^*$ interaction found in the global minimum.

The Bürgi-Dunitz[5] trajectory along the d_1 ($r(N_1\cdots C_{12})$, coordinate has been explored at MP2/6-311++G(2d,p) level for C1 to test some of the main characteristics of the $n\rightarrow\pi^*$ interaction in this complex including raw and BSSE complexation energy profiles. The results are summarized in Figure 5 and Table S19. As shown in figure 5, the stabilization energy due to this $n\rightarrow\pi^*$ delocalization is predicted to be highly dependent on d_1, being this interaction stronger for shorter distances. It has significant values for d_1 < 3.5 Å and for the r_0 structure (d_1=2.855 Å), the calculated stabilization energy is 10.4 kJ/mol. This is comparable for example to that obtained for GABA[13] with a similar value of the d_1 distance.

The experimental data do not provide direct evidence of other $n \rightarrow \pi^*$ interaction signatures like pyramidalization of FA. The *ab initio* calculations on the dependence of the deformation parameter Δ (see Figure 5) with d_1 predict some degree of pyramidalization of the carbonyl group for short distances $r(N_1 \cdots C_{12})$ (d_1 <3 Å), to some extent comparable to the dependence predicted according to the Bürgi-Dunitz model).[5] For the r_0 distance (d_1=2.855 Å), Δ is predicted to be only 0.004 Å while from the Bürgi-Dunitz model takes a slightly higher value, Δ = 0.009 Å (see Table S19).

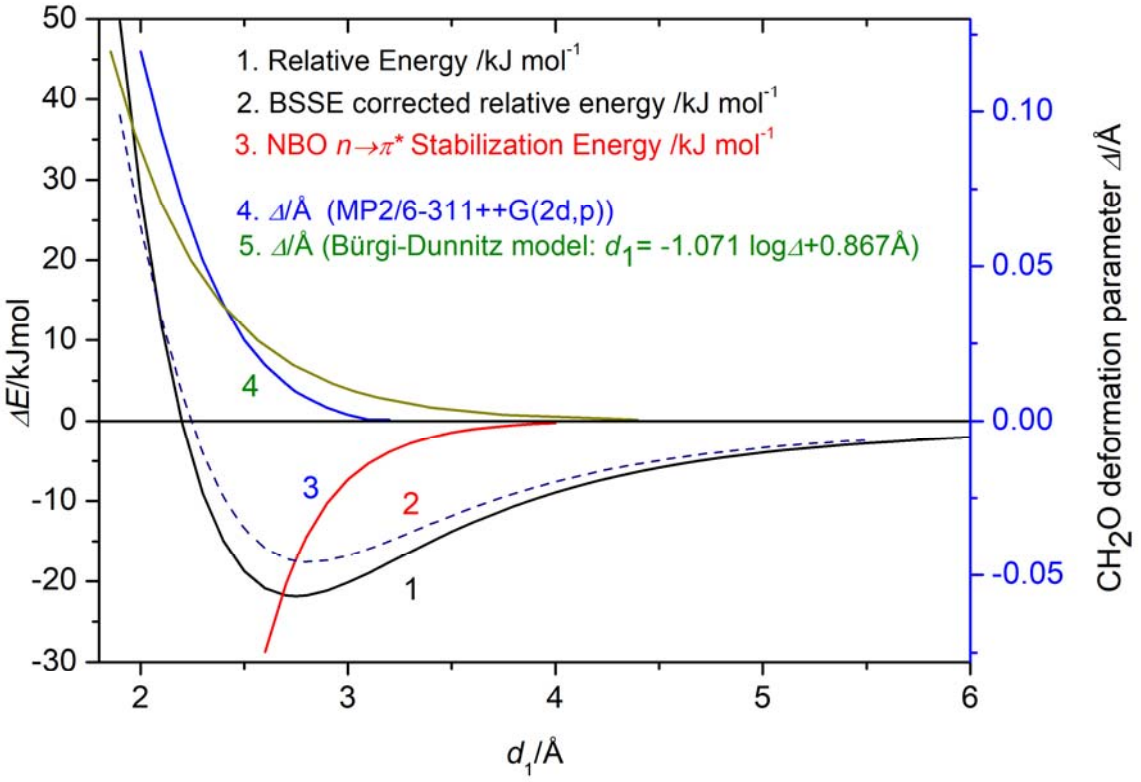

Figure 5. Results of the analysis of the Bürgi-Dunitz trajectory along the d_1 coordinate (see Figure 1). Curve 1 shows the variation of the calculated electronic energy relative to the configuration with d1 > 40 Å; curve 2 shows the BSSE corrected energy profile; curve 3 shows the dependence of the NBO stabilization energy due to n→π* interaction.; curve 4 gives the predicted ab initio dependence of the parameter Δ related to CH_2O pyramidal deformation; curve 5, shows the dependence of Δ according to the Bürgi-Dunitz model

The $n\rightarrow\pi^*$ interaction coexists with a weak C-H···O HB. This is not surprising since it has been reported that such interactions are often complemented by additional weak interactions to vicinal C-H bonds.[3,19] The geometry of the HB, distance r($H_7\cdots O_{13}$) = 2.53 Å and angles $\angle C_{12}O_{13}H_7$ = 94.7º, $\angle C_3H_7O_{13}$= 128º and $\angle H_{14}C_{12}O_{13}H_7$ = 90º indicate, according to general considerations,[38] that this is a very weak HB. As discussed previously, the NBO results corroborate this conclusion. The C-H···N and C-H···O HBs in C3 conformer are, according to NBO calculations, stronger to C-H···O HBs in C1, due to a more favorable geometry. However the $n\rightarrow\pi^*$ interaction in C1 is predicted to be stronger than both C-H···N and C-H···O HBs of conformer C3. Thus, PY-FA adduct formation seems to be clearly dominated by the $n\rightarrow\pi^*$ interaction.

To summarize, the experimental structure of PY-FA is consistent with its formation through an $n\rightarrow\pi^*$ interaction. Two of the signatures (i) and (ii) of the $n\rightarrow\pi^*$ interactions[4] are apparent from this structure. The N atom is in the plane bisecting the HCH angle (C_s symmetry). The distance r(N···C) is 2.844(6) Å, shorter than the sum of van der Waals radii, 3.25 Å. The Burgi-Dunitz angle ∠N···C=O is 102.8(6)º, within the predicted range of 107±10º. Theoretical calculations predict that the $n\rightarrow\pi^*$ is by far the strongest donor→acceptor intermolecular interaction existing in any possible conformer of this adduct. A small deformation of the carbonyl group is also predicted. The subtle changes in the ^{14}N quadrupole coupling tensor of PY[39] (see Table S17) associated to the formation of the adduct might be a probe for the effects of the $n\rightarrow\pi^*$ electron density delocalization affecting to the electronic environment of the N atom. However, the errors quoted for the principal elements are still too high to draw any firm conclusion about this.

In conclusion, the investigation of the rotational spectra of PY–FA and of its isotopologues lead to the irrefutable conclusion that it can be considered as an n→π* charge transfer complex. This

is, to our knowledge, the first time that this kind of n→π* interaction, first described in the pioneering papers of Bürgi and Dunitz,[5–7] is observed and described through the rotational study of a molecular complex.

ASSOCIATED CONTENT

Supporting Information. Summary of the ab initio results, determined rotational parameters and measured experimental frequencies, complete structures.

AUTHOR INFORMATION

E Mail Adresses: sblanco@qf.uva.es; jclopez@qf.uva.es.

The authors declare no competing financial interests.

ACKNOWLEDGMENT

The authors acknowledge the Ministerio de Economía y Competitividad (Grant CTQ2016-75253-P) for financial support.

REFERENCES

(1) Jeffrey, G. A. *An Introduction to Hydrogen Bonding*; Topics in Physical Chemistry - Oxford University Press; Oxford University Press, 1997.

(2) Steiner, T. The Whole Palette of Hydrogen Bonds. *Angew. Chem. Int. Ed* **2002**, *41*, 48–76.

(3) Paulini, R.; Müller, K.; Diederich, F. Orthogonal Multipolar Interactions in Structural Chemistry and Biology. *Angew. Chemie Int. Ed.* **2005**, *44*, 1788–1805.

(4) Newberry, R. W.; Raines, R. T. The n →π* Interaction. *Acc. Chem. Res.* **2017**, *50*, 1838–1846.

(5) Burgi, H.; Dunitz, J.; Shefter, E. Geometrical Reaction Coordinates. II. Nucleophilic Addition to a Carbonyl Group. *J. Am. Chem. Soc.* **1973**, *587*, 5065–5067.

(6) Bürgi, H. B.; Dunitz, J. D.; Lehn, J. M.; Wipff, G. Stereochemistry of Reaction Paths at Carbonyl Centres. *Tetrahedron* **1974**, *30*, 1563–1572.

(7) Bürgi, H. B.; Dunitz, J. D.; Shefter, E.; IUCr. Chemical Reaction Paths. IV. Aspects of O.C = O Interactions in Crystals. *Acta Crystallogr. Sect. B* **1974**, *30*, 1517–1527.

(8) DeRider, M. L.; Wilkens, S. J.; Waddell, M. J.; Bretscher, L. E.; Weinhold, F.; Raines, R. T.; Markley, J. L. Collagen Stability: Insights from NMR Spectroscopic and Hybrid Density Functional Computational Investigations of the Effect of Electronegative Substituents on Prolyl Ring Conformations. *J. Am. Chem. Soc.* **2002**, *124*, 2497–2505.

(9) Hinderaker, M. P.; Raines, R. T. An Electronic Effect on Protein Structure. *Protein Sci.* **2003**, *12*, 1188–1194.

(10) Singh, S. K.; Das, A. The n → Π* Interaction: A Rapidly Emerging Non-Covalent Interaction. *Phys. Chem. Chem. Phys.* **2015**, *17*, 9596–9612.

(11) Improta, R.; Benzi, C.; Barone, V. Understanding the Role of Stereoelectronic Effects in Determining Collagen Stability. 1. A Quantum Mechanical Study of Proline, Hydroxyproline, and Fluoroproline Dipeptide Analogues in Aqueous Solution. *J. Am. Chem. Soc.* **2001**, *123*, 12568–12577.

(12) Hinderaker, M.; Raines, R. An Electronic Effect on Protein Structure. *Protein Sci.* **2003**, *12*, 1188–1194.

(13) Blanco, S.; López, J. C.; Mata, S.; Alonso, J. L. Conformations of γ-Aminobutyric Acid

(Gaba): The Role of the N→π* Interaction. *Angew. Chemie Int. Ed.* **2010**, *49*, 9187–9192.

(14) Lesarri, A.; Cocinero, E. J.; López, J. C.; Alonso, J. L. Shape of 4(S)- and 4(R)-Hydroxyproline in Gas Phase. *J. Am. Chem. Soc.* **2005**, *127*, 2572–2579.

(15) Sanz, M. E.; Lesarri, A.; Peña, M. I.; Vaquero, V.; Cortijo, V.; López, J. C.; Alonso, J. L. The Shape of β-Alanine. *J. Am. Chem. Soc.* **2006**, *128*, 3812–3817.

(16) Bird, R. G.; Vaquero-Vara, V.; Zaleski, D. P.; Pate, B. H.; Pratt, D. W. Chirped-Pulsed FTMW Spectra of Valeric Acid, 5-Aminovaleric Acid, and γ-Valerolactam: A Study of Amino Acid Mimics in the Gas Phase. *J. Mol. Spectrosc.* **2012**, *280*, 42–46.

(17) Cabezas, C.; Alonso, J. L.; López, J. C.; Mata, S. Unveiling the Shape of Aspirin in the Gas Phase. *Angew. Chemie Int. Ed.* **2012**, *51*, 1375–1378.

(18) Choudhary, A.; Kamer, K. J.; Raines, R. T. An N→π* Interaction in Aspirin: Implications for Structure and Reactivity. *J. Org. Chem.* **2011**, *76*, 7933–7937.

(19) Pérez, C.; Neill, J. L.; Muckle, M. T.; Zaleski, D. P.; Peña, I.; López, J. C.; Alonso, J. L.; Pate, B. H. Water-Water and Water-Solute Interactions in Microsolvated Organic Complexes. *Angew. Chemie Int. Ed.* **2015**, *54*, 979–982.

(20) Gou, Q.; Feng, G.; Evangelisti, L.; Caminati, W. Lone-Pair···π Interaction: A Rotational Study of the Chlorotrifluoroethylene-Water Adduct. *Angew. Chem. Int. Ed. Engl.* **2013**, *52*, 11888–11891.

(21) Gou, Q.; Spada, L.; Geboes, Y.; Herrebout, W. A.; Melandri, S.; Caminati, W. N Lone-Pair□π Interaction: A Rotational Study of Chlorotrifluoroethylene□ammonia. *Phys. Chem. Chem. Phys.* **2015**, *17*, 7694–7698.

(22) Calabrese, C.; Gou, Q.; Maris, A.; Caminati, W.; Melandri, S. Probing the Lone Pair···π-Hole Interaction in Perfluorinated Heteroaromatic Rings: The Rotational Spectrum of Pentafluoropyridine·Water. *J. Phys. Chem. Lett.* **2016**, 1513–1517.

(23) Weinhold, F.; Landis, C. R. *Valency and Bonding*; Cambridge University Press: Cambridge, 2005.

(24) Tandon, R.; Unzner, T.; Nigst, T. A.; De Rycke, N.; Mayer, P.; Wendt, B.; David, O. R. P.; Zipse, H. Annelated Pyridines as Highly Nucleophilic and Lewis Basic Catalysts for Acylation Reactions. *Chem. A Eur. J.* **2013**, *19*, 6435–6442.

(25) Mandai, H.; Fujii, K.; Yasuhara, H.; Abe, K.; Mitsudo, K.; Korenaga, T.; Suga, S. Enantioselective Acyl Transfer Catalysis by a Combination of Common Catalytic Motifs and Electrostatic Interactions. *Nat. Commun.* **2016**, *7*, 11297.

(26) Boys, S. F.; Bernardi, F. The Calculation of Small Molecular Interactions by the Differences of Separate Total Energies. Some Procedures with Reduced Errors. *Mol. Phys.* **1970**, *19*, 553–566.

(27) Gordy, W.; Cook, R. L. *Microwave Molecular Spectra*; Wiley-Interscience: New York, 1984; Vol. 11.

(28) Pickett, H. M. The Fitting and Prediction of Vibration-Rotation Spectra with Spin Interactions. *J. Mol. Spectrosc.* **1991**, *148*, 371–377.

(29) Watson, J. K. G. Aspects of Quartic and Sextic Centrifugal Effects on Rotational Energy Levels. In *Vibrational Spectra and Structure a Series of Advances, Vol 6*; Durig, J. R., Ed.; Elsevier: New York, 1977; pp 1–89.

(30) Ye, E.; Bettens, R. P. a.; De Lucia, F. C.; Petkie, D. T.; Albert, S. Millimeter and Submillimeter Wave Rotational Spectrum of Pyridine in the Ground and Excited Vibrational States. *J. Mol. Spectrosc.* **2005**, *232*, 61–65.

(31) Bocquet, R.; Demaison, J.; Poteau, L.; Liedtke, M.; Belov, S.; Yamada, K. M. T.; Winnewisser, G.; Gerke, C.; Gripp, J.; Köhler, T. The Ground State Rotational Spectrum of Formaldehyde. *J. Mol. Spectrosc.* **1996**, *177*, 154–159.

(32) Kraitchman, J. Determination of Molecular Structure from Microwave Spectroscopic Data. *Am. J. Phys.* **1953**, *21*, 17–24.

(33) Kisiel, Z. Least-Squares Mass-Dependence Molecular Structures for Selected Weakly Bound Intermolecular Clusters. *J. Mol. Spectrosc.* **2003**, *218*, 58–67.

(34) Millen, D. J. Determination of Stretching Force Constants of Weakly Bound Dimers from Centrifugal Distortion Constants. *Can. J. Chem.* **1985**, *63*, 1477–1479.

(35) Balle, T. J.; Campbell, E. J.; Keenan, M. R.; Flygare, W. H. A New Method for Observing the Rotational Spectra of Weak Molecular Complexes: KrHCl. *J. Chem. Phys.* **1980**, *72*, 922–932.

(36) Ruoff, R. S.; Klots, T. D.; Emilsson, T.; Gutowsky, H. S. Relaxation of Conformers and Isomers in Seeded Supersonic Jets of Inert Gases. *J. Chem. Phys.* **1990**, *93*, 3142–3150.

(37) Glendening, E. D.; Badenhoop, J. K.; Reed, A. E.; Carpenter, J. E.; Bohmann, J. A.; Morales, C. M.; Weinhold, F. Nbo 5.9. *Theor. Chem. Institute, Univ. Wisconsin, Madison* **2009**.

(38) Steiner, T. Unrolling the Hydrogen Bond Properties of C–H···O Interactions. *Chem.*

Commun. **1997**, No. 8, 727–734.

(39) Heineking, N.; Dreizler, H.; Schwarz, R. Nitrogen and Deuterium Hyperfine Structure in the Rotational Spectra of Pyridine and [4-D] Pyridine. *Zeitschrift fur Naturforsch.* **1986**, *41a*, 1210–1213.